JOURNAL OF CATALYSIS 28, 183–199 (1973)

An Experimental Study of Electronic Factors in the Dehydrogenation of Ethanol on Thin Film ZnO

DENNIS P. McARTHUR* AND HARDING BLISS

Department of Engineering and Applied Science, Yale University, New Haven, Connecticut 06520

AND

JOHN B. BUTT†

Department of Chemical Engineering, Northwestern University, Evanston, Illinois 60201

Received Oct. 12, 1971

Electron transfer mechanisms involved in the adsorption and catalytic dehydrogenation of ethanol on thin-film zinc oxide were investigated. A primary objective was to measure changes in the electrical conductivity of the catalyst resulting from adsorption and surface reaction processes, and to study the effects of electrical fields in activity, selectivity and adsorptive capacity of the zinc oxide. At low temperatures (<200°C) adsorption–conductivity experiments indicated that ethanol adsorbs as an electron donor, and at higher temperatures where appreciable surface reaction occurred (>225°C) the composite adsorbate layer, ethanol plus reaction products, also behaved as a donor. Individual components hydrogen, water, and ethylene adsorb as weak donors at 150°C, while acetaldeyde adsorbs as a strong acceptor under such conditions. These results indicate that under reaction conditions the adsorbed layer consists primarily of ethanol and hydrogen product, the reaction step involving immediate desorption of acetaldehyde product. Field-effect experiments were conducted for temperatures from 100 to 250°C. The activity and selectivity of the catalyst were not changed by external dc fields up to 10^4 V/cm, however strong effects of the field on the adsorptive capacity of the catalyst were observed for $T \geq 200$°C. These results indicate that the rate-limiting step is not affected by the surface concentration of free electrons and also suggests that the overall reaction rate is not limited by adsorption-desorption steps.

INTRODUCTION

In the temperature range to 400°C, zinc oxide is a selective catalyst for alcohol dehydrogenation and our interest here is the study of some of the electronic factors involved in this typical (but not simple) reaction on the *n*-type semiconductor catalyst. Three types of experiments are involved; reaction-rate studies, adsorption–conductivity studies, and external electric-field effect studies. Conductivity measurements are reported for the ZnO surface on exposure to each of the species involved in the dehydrogenation reaction both at low temperatures and under reaction conditions. The electric field studies are meant to determine the effects of external dc fields on the activity, selectivity (*vis a vis* dehydration), and adsorptive capacity of ZnO in this reaction.

* Present address: Union Oil Co. of California, Brea, California 92621.

† To whom correspondence should be addressed.

Adsorption Studies

Several prior studies have been devoted to the measurement of changes in the electrical properties of ZnO, particularly conductivity, accompanying the adsorption of the substances involved in the dehydrogenation reaction.

Hydrogen chemisorption is generally reported to be donor type (*1–7*) with conductivity increasing with temperature and surface coverage. At temperatures below about 110°C, conductivity changes are very small (*4–6*) and this has been explained in terms of covalent bonding of molecular H_2 (*5*); at higher temperatures large changes in conductivity are observed resulting from dissociative adsorption and the formation of surface donors. Conductivity changes at high temperatures appear to be reversible, but there is disagreement on whether reduction of the surface occurs under such conditions (*4, 6*).

Some confusion exists as to the nature of ethanol chemisorption. Bhattacharyya *et al.* (*5, 8*), in two separate investigations with pelleted ZnO at temperatures up to 180°C, have measured both increases and decreases in conductivity on ethanol chemisorption. The discrepancy is attributed to the presence of chemisorbed O_2 in one case, leading to *p*-type behavior and a decrease in conductivity on ethanol chemisorption. Donor chemisorption was observed on a more severely outgassed sample. Hydrogen chemisorption was donor type in both cases, however, so the explanation involving an inversion from *n*-type to *p*-type behavior is questionable. Bielanski and coworkers (*9, 10*) have studied adsorption of ethanol–water mixtures at reaction conditions and report donor chemisorption. Quantitative interpretation of these results is difficult since the measured changes reflect the composite effect of all species on the surface and even at low temperatures water was added in great excess to prevent pyrolysis and retard the dehydration reaction.

Ethylene adsorption has been investigated on stoichiometric and nonstoichiometric ZnO (*7*); for the former, a conductivity increase of 10^3 was measured at 150°C, for the latter a fourfold decrease. For stoichiometric oxide, the adsorption is visualized as a charge-transfer step giving $C_2H_4^+$ $O^{2-} + e^-$, and for nonstoichiometric material, there is a localization of electrons but no charge transfer. Two configurations are suggested in this latter case:

$$-S_1-CH_2-CH_2-S_1 \quad \text{and} \quad S_2-CH—CHS_2$$

where S_1 sites are O^- ions and S_2 sites are Zn_i^+ or a $(Zn_i^+–O^-)$ pair.

Acetaldehyde and water adsorption have been reported only by Bielanski *et al.* (*9, 10*), and the information is not complete. No acetaldehyde–ZnO data are given, but donor adsorption on *p*-type NiO is observed. Water adsorption is reported not to affect the conductivity of ZnO but the experiments, as mentioned above, involved water-saturated surfaces.

Field effects. The influence of external fields on the thermodynamics of absorbate layers was studied theoretically as long ago as 1935 (*11*), but experimental work dates from 1960. Studies of adsorptive capacity and reaction-rate modification have been reported; methods using external electrodes (external field method) or using the semiconductor itself as one of the electrodes (field effect method) have been developed, differing primarily in the fact that the specimen does not remain electrically neutral in the latter method. Adsorption experiments, all with dc fields, have been reported for O_2 on ZnO films (*12*), O_2 on epitaxial films of HgS on NaCl (*13*), and for CH_3 OH on germanium crystals (*14*). An example of such effects is the O_2–ZnO system (*12*): The induction of a negative surface charge on ZnO increased its capacity for O_2 adsorption at 300° K and a positive charge decreased capacity, in accord with the view that O_2 adsorbs on ZnO as an electron acceptor, O_2^- or O^-.

Catalytic reactions studied with dc fields include isopropanol dehydration on TiO_2 films (*15*), CH_4 oxidation on ZnO and ZnO–Cu_2O pastes (*16*), alcohol–O_2 reactions on Ag films (*17*), NH_3 synthesis on promoted Fe (*18*), and ethanol dehydrogenation on ZnO–Cu_2O wafers (*19*). With

ac fields CO oxidation on NiO disks (*20*) and benzene hydrogenation on brass and Ni-plated brass (*21*) have been investigated. In each instance some combination of field polarity and field strength for dc experiments, or frequency and field strength for ac experiments, was found to enhance reaction rate, and other combinations to depress the rate. Changes in selectivity have also been noted (*17*). A complete survey of the literature in this area has been given by McArthur (*22*).

The only study relating to the present work is that of Ivankiv *et al.* (*19*), who measured relative conductivity changes, $\Delta\sigma/\sigma_0$, and acetaldehyde yield, $\Delta k/k_0$, as a function of polarity and magnitude of applied field for ethanol–water feeds (1 atm, 250°C) over a ZnO–1%Cu_2O catalyst. Fields of $\pm 3.5 \times 10^5$ V/cm were employed; $(\Delta\sigma/\sigma_0)$ decreased with positive catalyst potentials and increased with negative potentials. These variations were linear with field strength and of small magnitude, about 3% in $\Delta\sigma/\sigma_0$. The acetaldehyde yield was markedly increased under positive potentials and inhibited to a lesser extent by negative ones. An increase of $\Delta k/k_0$ of $+0.2$ was determined at 2×10^5 V/cm, and a decrease of -0.05 at -2×10^5 V/cm. The electronic properties of the ZnO–Cu_2O are substantially different from those of ZnO, and it turns out that these results are not very similar to what has been obtained in the present study.

Experimental

Apparatus

A flow system of relatively standard design was used for all experiments. Ethanol was supplied to the reactor from an adiabatic vaporizer, and reactor effluent passed through a condenser. A continuous N_2 sweep entered the effluent line just above the condenser to prevent accumulation of noncondensibles and the unreacted ethanol was collected and its flow rate measured. Samples of reactor feed and effluent were analyzed by a chromatographic method described by Dabrowski *et al.* (*23*). In adsorption experiments acetaldehyde and water were supplied from a separate feed system using nitrogen saturated with the given adsorbate. Hydrogen and ethylene were supplied from separate gas feed systems, as was nitrogen purge stream (*22*).

The design of the reactor itself is of interest. A cylindrical baffle-disk arrangement permitted the use of thin film catalysts, the application of external electric fields normal to the catalytic surfaces, and measurement of changes in the electrical conductivity of the catalyst accompanying chemisorption or reaction over a wide range of temperatures. The reactor body consisted of a 4 in. i.d. by 24 in. long flanged Kimax glass pipe fitted with two end caps reducing to ¾ in. for feed and effluent lines. Iron–constantan thermocouples were placed on the outer surfaces at each end and at three points along the active length of the reactor. The entire assembly was wrapped with high-temperature heating tapes and mounted vertically within an insulated enclosure. The reactor internal configuration consisted of preheating and reaction sections, with reactant

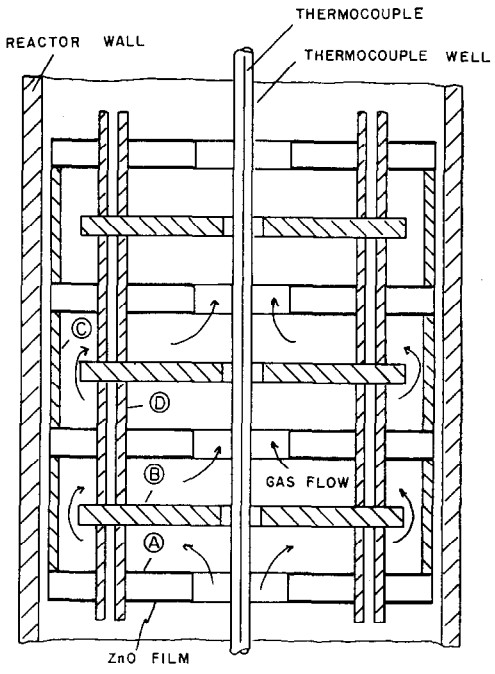

FIG. 1. Internal configuration of baffle-disk reactor.

flow upward through the reactor. The reaction zone contained a stacking of alternate catalyst support disks (A) and field disks (B), as shown on Fig. 1. These disks were separated and maintained parallel by spacing rings (C) and tubes (D). Temperature measurements were made with a movable thermocouple probe on the reactor axis. The catalyst support disks were Pyrex glass, while field disks were silver and were connected in parallel circuit by 0.010 in. diameter gold wire threaded through small radial holes drilled from the rim to the alignment holes. The geometry of support and field disks and of the electrical connections is shown on Fig. 2a. A special disk assembly was used for conductivity measurements. Two contact plates, each with two tungsten contact electrodes 0.040 in. in diameter were mounted upon the conductivity disk and this assembly was placed at the top of the reaction zone. The catalyst deposit on the conductivity disk, shown in Fig. 2b, unlike the deposits on the other catalyst disks, did not extend around the entire circumference. All external connections were made by enclosing the leads in fine, drawn-glass capillary tubes cemented in place within the exit line and passing through its wall.

The electronic apparatus included a ±5 kV dc, 500 mA Allen–Jones power supply for external field applications, a 500 V dc homemade power supply in series with high resistance (10^7–10^9 ohms) for current supply in conductivity measurements, an RCA WV-84A ammeter (0.01–1000 μA) for current measurements and a Kiethley

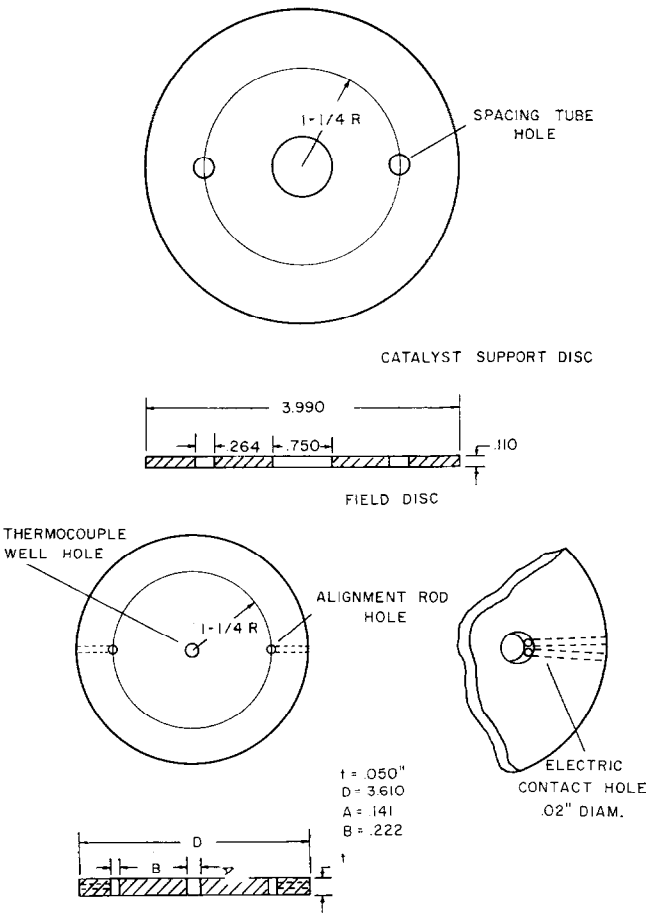

FIG. 2a. Catalyst support and field disk geometry.

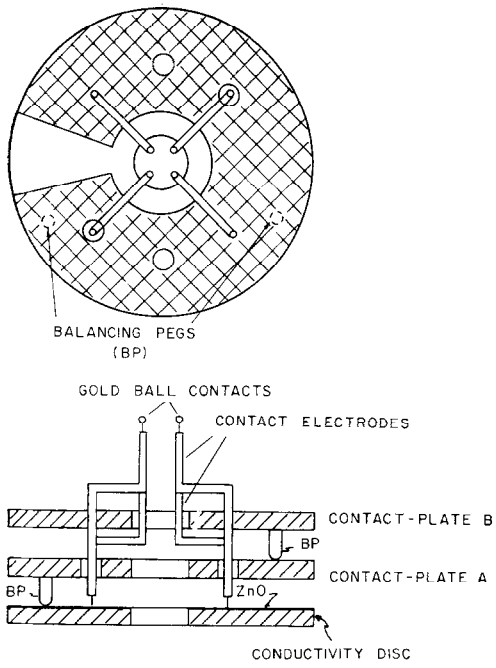

Fig. 2b. Conductivity disk and contact electrodes.

610B electrometer for voltage measurement in the conductivity experiments. An L and N 8686 millivolt potentiometer was employed for measurement of thermocouple outputs. Circuit diagrams for the application of electric field and for the measurement of ZnO film resistance are shown in Fig. 2c.

Materials

Gases used were prepurified-grade nitrogen (99.997%), C.P. ethylene (99.5%), prepurified hydrogen (99.95%) and ultra high-purity argon (99.9995%). All gases except argon for sputtering were dried by 5A sieves. Ethanol was USP-NF reagent grade, also predried by 5A sieves, and acetaldehyde was ACS reagent grade. Water was deionized and distilled. The gold wire and silver sheet used for fabrication of various gaskets and field disks was 99.95% in each case; zinc sheet, 99.98%, was used in preparation of the catalyst.

Catalyst

The catalyst was prepared by sputtering zinc films onto the glass support disks and subsequently oxidizing them in air at 410°C for 18.5 to 22.5 hr, about 20-fold the time required for complete oxidation at these conditions. Catalyst was deposited on both sides of 19 disks, on one side of two others, and on the conductivity disk as shown on Fig. 2b. The thickness of the ZnO film was determined gravimetrically to be 2950 ± 70 Å average with a range from 2650 to 3450 Å on the catalyst disks, and 3200 ± 100 Å on the conductivity disk. These results were confirmed by interferometric measurements. Total weight of the films was 527.1 ± 12.4 mg, and the total geometric exposed area of the films in the reactor was 3150 cm^2. X-ray diffraction analysis of a special sample of oxide gave crystallite sizes of 350, 390, and 380 Å for the 101, 002, and 100 planes, respectively. These results are generally in accord with the measurements of Seitz (*24*), including the effect of film thickness on crystallite size. The specific surface area was not measured directly but from the results of Rhodin (*25*) on similar materials it seems safe to assume roughness factors on the order of 2–3, giving area estimates from 1.5 to 3.0 m^2/g in the limit from nonporous to porous films. Resistance measurements were made at 22°C on the conductivity film in a nitrogen atmosphere using the four-point dc method. The catalyst behaved as an ohmic resistor over the range $1.2 \times 10^{-8} \leq I \leq 1.1 \times 10^{-6}$ Å and $0.8 \leq V \leq 76.1$ V dc with an average specific resistivity of 1490 ohm-cm.

Procedures

Some specific kinetic measurements for the dehydrogenation reaction at 250–400°C were made in a small differential pilot reactor using zinc oxide films on glass slides as the catalyst, the oxide layer being about 2850 Å thick. The substrate was broken into small irregularly shaped pieces of maximum dimension about 5 mm, giving a total exposed area of catalyst in the flow reactor of 414 cm^2 and a weight of 66.9 ± 0.9 mg. The catalyst was pretreated by exposure to dry nitrogen at reaction temperature. Reaction rates were determined from analysis

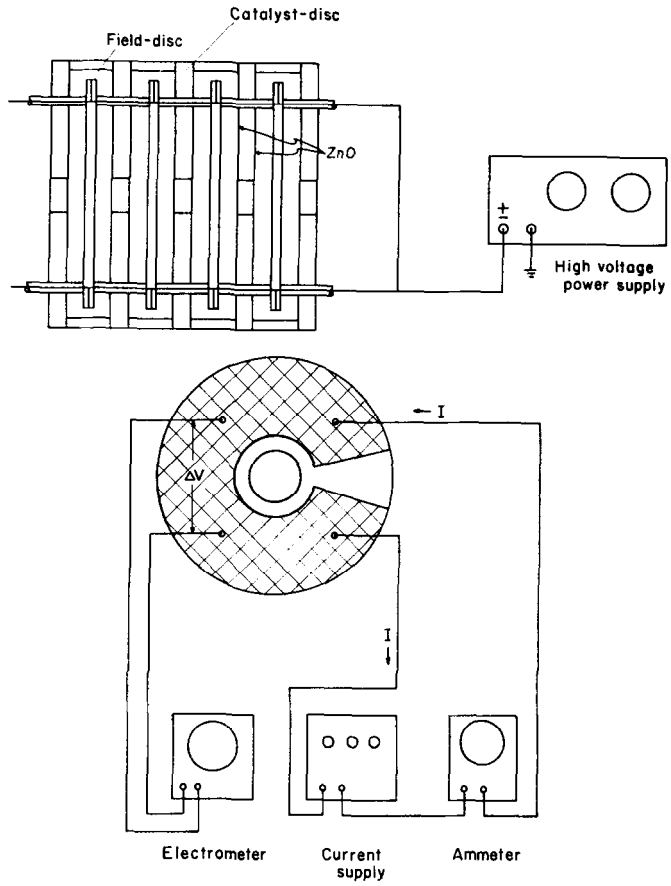

FIG. 2c. Schematic circuit diagrams for field application (top) and resistance measurements (bottom).

of the gaseous reactor effluent plus volumetric measurement of the flow rate of unreacted ethanol in the effluent. Conversions were always less than 6%, and reactant partial pressure was not varied in these experiments.

Experiments involving conductivity measurements or external fields were conducted with the baffle-disk reactor. Both two-point and four-point methods were used for conductivity measurement. In the two-point method, both voltage drop and current are measured between two contact probes, while the four-point method employs separate probes for current and voltage measurements. A high-impedance voltmeter was used (10^{14} ohm), since the resistances measured were as high as 10^{9} ohm.

Experiments

A basic series of experiments was run to determine conductivity changes accompanying chemisorption and dehydrogenation of ethanol on ZnO at 100–300°C, atmospheric pressure, and low conversion (<2%). The film resistance was first measured in a nitrogen atmosphere at reaction temperature, then ethanol flow started through the reactor. The adsorption was followed by continuous measurement of film resistance to steady state; a desorption cycle reversed this procedure. The ohmic behavior of the film was confirmed at both initial and final conditions; normal measurements of catalyst film resistance employed currents from 10^{-5} to 10^{-7} A to minimize resistance heating.

Reaction rates were measured from 100–350°C, both with and without externally applied fields, in the same series of experiments. The reactant partial pressure was 1 atm, and feed rate was used to control conversion which, in this case, was always $<6\%$. At each temperature the reaction rate with no external field was determined over a range of feed rates, then determined in the presence of an external field at the highest feed rate. Positive and negative potentials up to 5000 V were employed, corresponding to maximum field strengths of $\pm 1.2 \times 10^4$ V/cm.

A series of experiments was also conducted to determine field effects on ethanol chemisorption on ZnO. These were similar to the adsorption-reaction experiments although at lower temperatures to preclude significant reaction. Chemisorption was initiated in the absence of the field; near equilibrium, as indicated by resistance measurements, the field was applied and maintained for a period of time. Resistance measurements could not be made during field application, but were resumed after termination of the field and continued again to the steady state. These experiments were carried out at 100, 150, 201, and 250°C with fields of ±5 kV dc.

A final set of experiments measured and compared changes in the catalyst conductivity on individual adsorption of ethanol, acetaldehyde, ethylene, hydrogen, and water at 150°C. In addition, some sequences of adsorption were also studied: ethanol–acetaldehyde, ethanol–hydrogen, ethanol–ethylene, ethanol–water, and the reverse sequences, i.e., acetaldehyde–ethanol, etc.

Results and Discussion

Catalytic Activity

Specific rate measurements were obtained both from the pilot reactor and the reaction–conductivity experiments with the baffle-disk reactor. A detailed reaction kinetic study was not an objective, so the experimentation was limited to 100–400°C and reactant partial pressure of 1 atm. The kinetics so measured are well correlated by a zero-order law and the absolute values of specific rate determined in the two experiments are in good agreement although the activation energies differ by about 4 kcal/mole. Major results are summarized on Fig. 3. Measurable rates were obtained above 225°C; the catalyst was selective for dehydrogenation although ethylene, methane, ethane, carbon dioxide, and water were all detected in small amounts in the effluent indicating parallel dehydration, acetaldehyde decomposition, and possibly ethylene hydrogenation, all of which have been reported on ZnO (*7*, *10*, *26*). The compensation between the two catalysts is probably the result of somewhat different stoichiometry and crystallite size arising from differing oxidation times for the sputtered zinc, 48 hr for curve I and 20 hr for II.

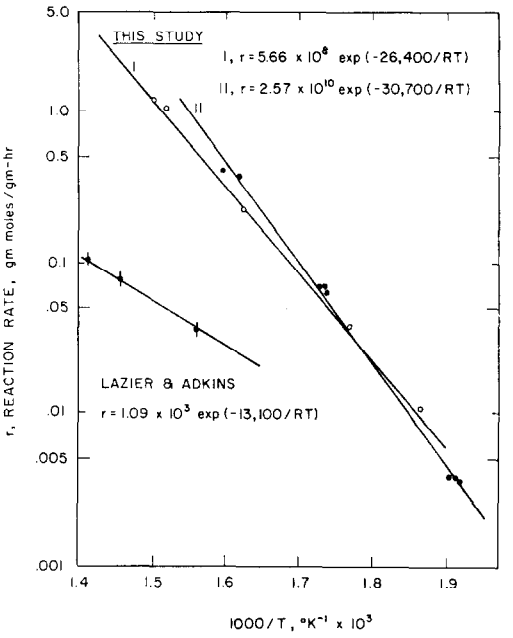

FIG. 3. Arrhenius correlation of zero-order rate constants for ethanol dehydration on ZnO at 225–400°C. Curve I, Differential reactor data; Curve II, Integral reactor data.

Lazier and Adkins (*27*) report an activation energy of 13.1 kcal/mole for the zero-order reaction on a tableted catalyst. The present results, with activation energies roughly twice this value, indicate a diffusion limitation in their measured rates.

Chemisorption and Dehydrogenation of Ethanol

The chemisorption–conductivity results fall into two temperature ranges. Below 225°C the catalyst is essentially inactive and conductivity changes are due entirely to ethanol chemisorption; above this temperature conductivity changes reflect also the influence of reaction products acetaldehyde and hydrogen.

Under all conditions exposure of the catalyst surface to ethanol resulted in an increase in the conductivity (decrease in resistance) which increased in magnitude with temperature as shown on Fig. 4. Experimental resistance measurements are given on the figures although it will be convenient to discuss results in terms of conductivity. Ethanol adsorption at 201°C increased conductivity by a factor of 10 with an equilibrium time of 80–90 min (Fig. 4, top). The very pronounced temperature effect on conductivity is shown on the bottom of Fig. 4; at 300°C conductivity increased by a factor of 230 and the equilibrium time reduced to 3 min.* The kinetics of these adsorptions is complex. Even at lower temperatures without the complication of surface reaction, changes in conductivity do not follow relaxation time correlations such as those employed by Liashenko and Litorchenko (*28*). This applies to the results with sorbates other than ethanol as well. However, the adsorptions were found to follow an Elovich rate

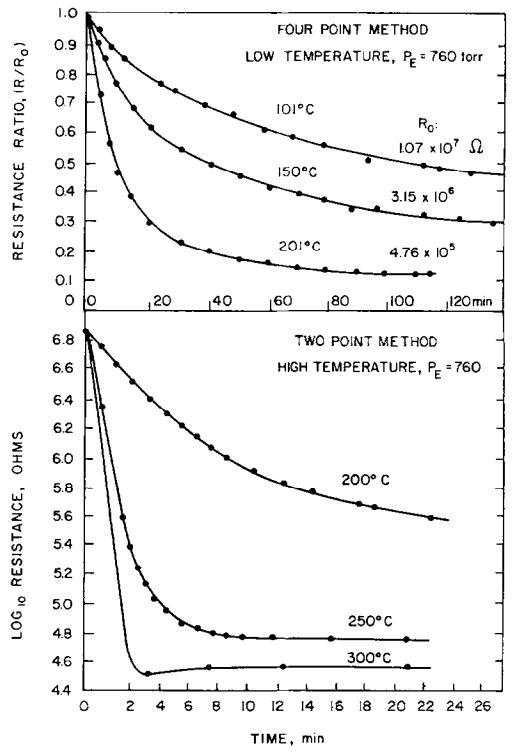

FIG. 4. Conductivity changes of ZnO film on ethanol chemisorption.

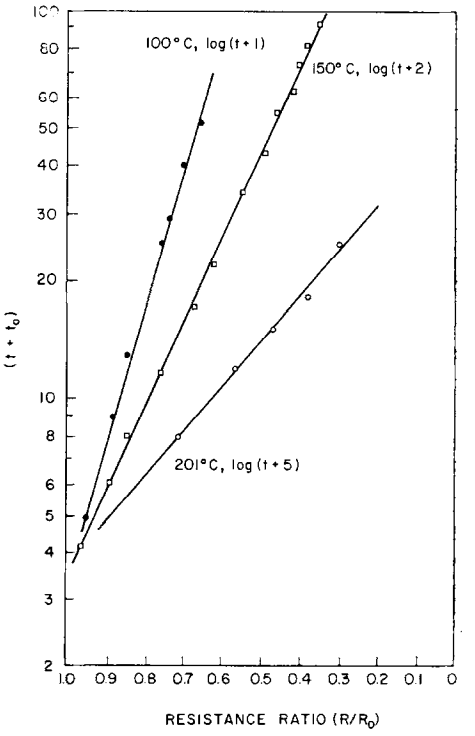

FIG. 5. Elovich correlation of ethanol chemisorption kinetics.

* Measurements at lower temperatures were made using the four-point method, but equipment failure necessitated use of the two-point method for all subsequent measurements. Both methods were used at the single temperature of 200°C; the results are not identical because the contact resistances associated with the two-point method are extremely difficult to reproduce. However, results given by the two methods are qualitatively the same so the trends discussed do not need to be segregated according to experiment.

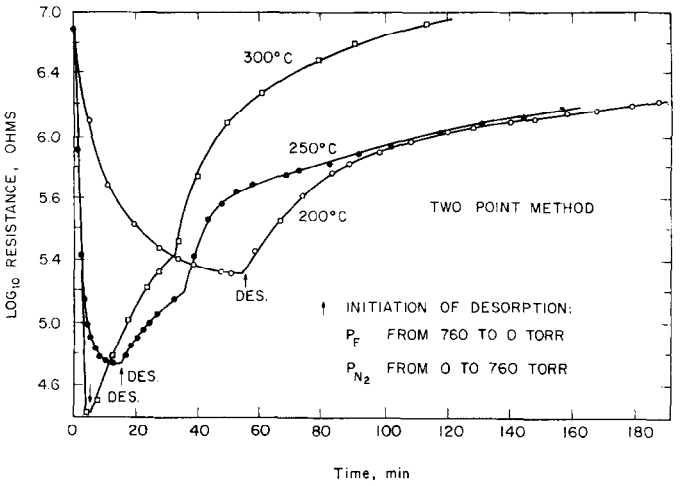

FIG. 6. Adsorption and subsequent desorption of ethanol on ZnO in the temperature range from 200–300°C. *Arrows indicate initiation of desorption into nitrogen atmosphere.*

law for a time period corresponding to resistance changes of about half the initial value. An example of such a correlation for the ethanol adsorption data of Fig. 4 is given in Fig. 5. Taylor and Thon (*29*) have also reported Elovich kinetics for hydrogen chemisorption on ZnO.

The conductivity changes measured were reversible; at 100 and 150°C the desorption was very slow with equilibrium occuring at 90 and 30 hr, respectively. Complete adsorption–desorption histories are shown on Fig. 6 for 200, 250, and 300°C. The desorption curves at the two higher temperatures where significant surface reaction takes place have a complex shape, suggestive either of desorption of two different absorbate species or, again, desorption of a single species from two different surface sites. The difference in desorption kinetics between 200 and 250°C is consistent with the appearance of surface reaction at about 225°C.

The conductivity increases on chemisorption and reaction of ethanol indicate that the adsorbate layer is an electron donor over the entire temperature range studied, with very strong interactions indeed at the higher temperatures. These results are in agreement with those of Bielanski *et al.* (*10*) regarding donor adsorption of ethanol on ZnO.

Field Effects on Ethanol Chemisorption

The charge transfer properties of ethanol chemisorption on ZnO indicate that external fields altering the surface concentration of free electrons should have a strong effect on rates and equilibria. In the results described here, the direction of the field was normal to the surface and was such that when the field disk was maintained at a negative potential, the concentration of free electrons at the exposed surface of the catalyst film was increased; resultant changes in conductivity are attributed to changes in coverage and in composition of the adsorbate layer.

Application of fields zero to ±5 kV dc in nitrogen atmosphere did not change catalyst conductivity, nor was the conductivity changed at 100°C in an ethanol atmosphere. A field effect was observed at 150°C with ethanol, however, as shown on Fig. 7, but only for negative fields, resulting in a substantial decrease in catalyst conductivity. The field effect here is apparently irreversible; it is seen that at the start of desorption the catalyst resistivity was higher than in the initial state and continues to increase with desorption. This desorption is complete after 5 hr vs the 30 hr required in experiments without fields at 150°C. The irreversibility appears to be

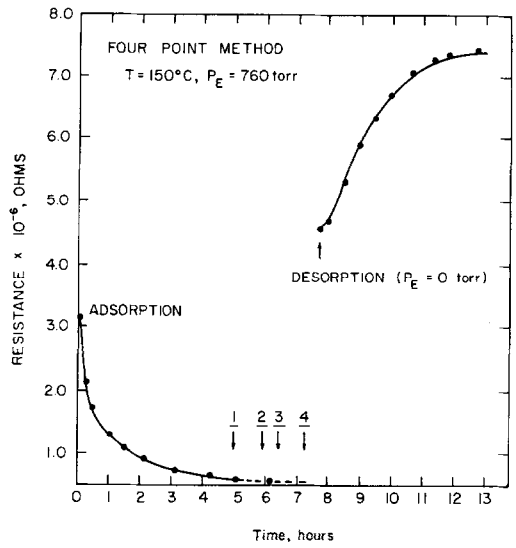

FIG. 7. Field effect on the adsorption of ethanol at 150°C. +5 kV field applied between 1 and 2. −5 kV field applied between 3 and 4. Dotted line segments indicate no resistance measurement made during this time period.

due to the trapping of a fraction of the conduction electrons in surface states, probably associated with valency unsaturated lattice O^- ions (holes), which also serve to decrease the conductivity. For an *n*-type material the hole concentration is greater at 150 than at 100°C, which may explain why the field effect was observed only at the higher temperature.

At 201°C negative fields again were found to produce substantial decreases in conductivity, and again positive fields gave no change. Desorption is strongly enhanced by the field and the ethanol readsorbed on removal of the field; the reproducibility of these effects is shown in Fig. 8, top. In Fig. 8, bottom, is given a comparison of identical runs, one with and one without application of a negative field showing that the field effect of 201°C is reversible. Substantial desorption occurs on application of the field, even in an ethanol atmosphere (point 1). When the desorption is allowed to occur into flowing nitrogen after removal of the field (point 2), a normal rate is obtained with the conductivity returning to its initial value as shown on the right hand side of the figure. The readsorption shown in the figure is due to the time lag between cessation of ethanol flow and introduction of nitrogen to the reactor and the appearance of nitrogen at the conductivity disk, which was located at the reactor outlet.

At 250°C, effects were noted with both positive and negative fields. Conductivity increases with positive fields indicated increased equilibrium chemisorption; these changes were apparently reversible, with desorption and return to initial conditions on termination of the field application. Negative fields produced the same results as 201°C, decreasing equilibrium chemisorption. These results are depicted in Fig. 9; the times required for return to equilibrium after application and removal of the positive and negative fields were 30 and 5 min, respectively.

If the change in equilibrium surface coverage produced by field application is proportional to the change in conductivity, then it would appear that ethanol is more strongly adsorbed at the higher temperatures. At 201°C, conductivity was altered at least 20-fold at −5 kV dc (Fig. 8, top) at 250°C by at least two-fold (Fig. 9). Further, the irreversibility of the field effect at 150°C disappears at higher temperatures. If the only consideration were the surface trapping, $e^- + O^- \rightarrow O^{2-}$, one would expect the irreversibility to persist and even grow more pronounced at higher temperatures. However, the field was applied after steady-state adsorption existed, and since ethanol adsorbs as a donor it is possible that the O^- surface traps could be filled with electrons from the ethanol. Thus, an explanation for the disappearance of irreversible field effects is the adsorption itself, which reversibly supplies sufficient electrons to fill existing surface traps at 201 and 250°C, but not at 150°C. The absence of any influence of positive fields below 250°C can be explained on the basis of surface coverage; at lower temperatures the surface is saturated and the retarding effect of a positive field on desorption would not be observed, while at higher temperatures the surface contains a significant number of unoccupied sites which the posi-

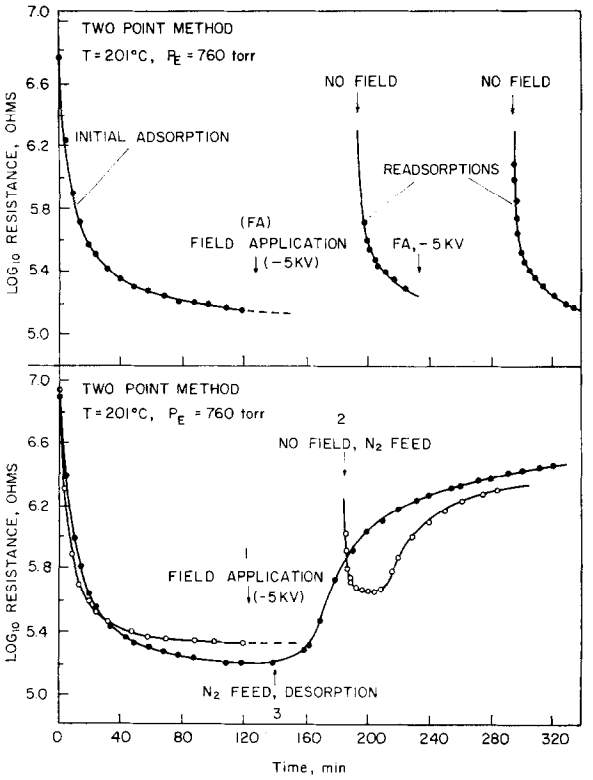

FIG. 8. (Top) Field effect on the adsorption of ethanol at 201°C, 5 kV field applied between arrows as indicated. (Bottom) Comparison of identical ethanol adsorption experiments with and without field. ●, Experiment with no field application, desorption initiated at 140 min; ○, experiment with application of 5 kV field from 120 to 190 min, desorption initiated at 190 min.

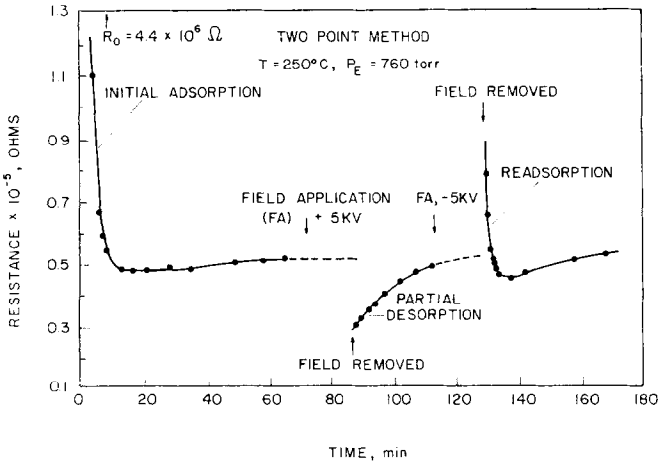

FIG. 9. Field effects on the adsorption of ethanol at 250°C. Sequential application of + and −5 kV fields showing enhancement of adsorption with the positive field and inhibition with the negative field. Dotted line segments indicate no resistance measurements made during this time period.

tive field would tend to reduce. The absence of any field effect, positive or negative, at 100°C is also explained in terms of not being sufficient to alter the condition of saturation surface coverage. This requires that ethanol coverage be large and essentially constant in the range 100–200°C, and this has been observed in the adsorption data of Bhattacharyya *et al.* (*19*) from 80 to 180°C at much lower adsorbate pressures (2–80 mm Hg). However, adsorption–conductivity experiments without field indicate relatively small conductivity changes for ethanol chemisorption at low temperatures, so it appears that two types of chemisorption occur: a strong interaction involving electron transfer between the adsorbate and the surface which predominates at high temperatures and leads to large conductivity changes, and a weak, perhaps electrostatic, interaction not involving electron transfer at lower temperatures.

Adsorption at 150°C

The changes in conductivity measured at higher temperatures as those on Fig. 4 may include contributions of reaction products present in the adsorbate layer. Accordingly, a knowledge of the interactions of each possible product with the surface under conditions of no reaction is desirable. In Fig. 10 are compared experimental adsorption–conductivity data for ethanol, water, ethylene, hydrogen and acetaldehyde. Water, ethylene, and hydrogen are all adsorbed as donors and their interactions both in terms of the magnitude of conductivity change and the rapidity of desorption (*22*) are weak compared to ethanol. The donor adsorption of hydrogen is in agreement with the literature (*1–7*), and the small interactions with water are consistent with the observations of Bielanski (*9*). Ethylene results, however, disagree with Bozon-Veruraz *et al.* (*7*), who reported weak acceptor adsorption on nonstoichiometric ZnO. Not shown in Fig. 10 is the fact that after the initial adsorption of hydrogen, a slower and nearly constant uptake ensued which extended over the entire exposure time of 3 hr. This is consistent with the results of Taylor and Thon

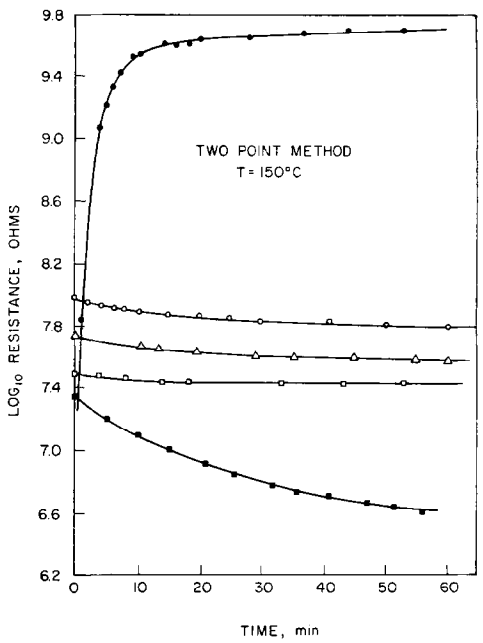

FIG. 10. Comparison of the conductivity changes of ZnO film on the adsorption of acetaldehyde, hydrogen, water, ethylene and ethanol at 150°C. ●, Acetaldehyde, P = 41 Torr, $R_0 = 1.84 \times 10^7\Omega$; ○, Hydrogen, P = 760 Torr, $R_0 = 9.57 \times 10^7\Omega$; △, Water, P = 22 Torr, $R_0 = 5.38 \times 10^7\Omega$; □, Ethylene, P = 760 Torr, $R_0 = 3.18 \times 10^7\Omega$; ■, Ethanol, P = 760 Torr, $R_0 = 2.23 \times 10^7\Omega$.

(*29*) and may be due to differing sites for H_2 chemisorption or to absorption (dissolution) into the ZnO lattice.

Acetaldehyde is adsorbed as an acceptor and, on the basis of the large magnitude of conductivity change and a very slow rate of desorption (*22*), its interaction with the surface is strong. Changes in conductivity accompanying the dehydrogenation reaction at higher temperatures indicate net donor adsorption, so in view of the strong acceptor behavior of acetaldehyde, it seems probable that this product is desorbed immediately upon formation. This hypothesis can be tested by examining the adsorption competition between participants in the reaction, so the interactions of some adsorbate pairs were studied separately. The most interesting of these is the ethanol–acetaldehyde system shown in Fig. 11. The top half shows that ethanol is readily adsorbed on ZnO previously ex-

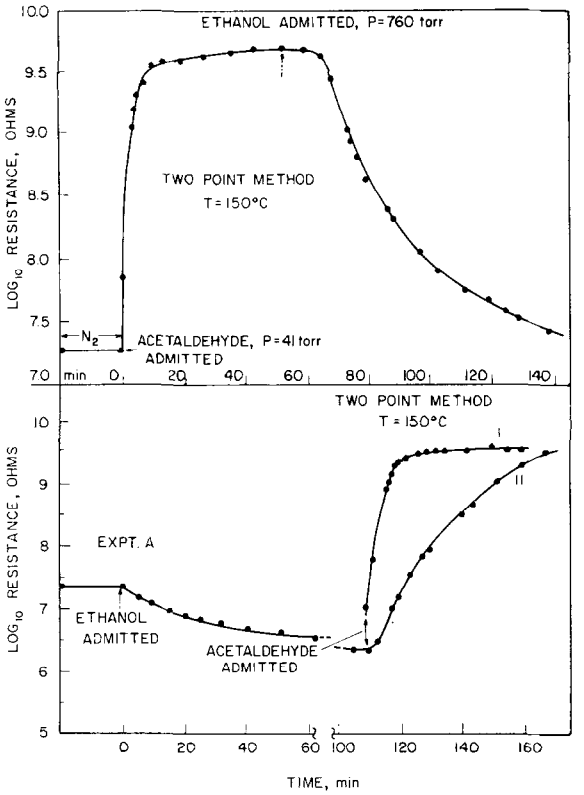

FIG. 11. Sequential adsorption experiments with acetaldehyde–ethanol (top), and ethanol–acetaldehyde (bottom). In the bottom: Experiment A, ethanol adsorption on fresh surface, P = 760 Torr; curve 1, acetaldehyde adsorption on fresh surface, P = 41 Torr; curve 2, acetaldehyde adsorption on equilibrated surface from Expt A, P = 35 Torr.

posed to acetaldehyde, and this adsorption changes conductivity by a factor of 450 vs a factor of 10 for ethanol adsorption on a nitrogen-equilibrated surface (Fig. 10). This large change can be due either to displacement of acetaldehyde by ethanol or by the acetaldehyde in some way increasing the capacity of the surface for the strong donor adsorption of ethanol. In the lower half of the figure, we see that acetaldehyde is also taken up on an ethanol-covered surface and the resulting magnitude of conductivity change is about the same as on a nitrogen-equilibrated surface. However, the rate of adsorption is substantially inhibited by the presence of the alcohol, as shown by the comparison between curves I and II at the right of the figure. Other experiments of this type (*22*) indicated that ethanol adsorption on surfaces equilibrated previously with 1 atm ethylene or hydrogen is the same as for a nitrogen-equilibrated surface, while with water there is a small interaction involving a change in conductivity by a factor of 5.5 vs 10 for the nitrogen-equilibrated surface. This indicates that ethanol and water compete to a small extent for the same adsorption sites. Conversely, ethylene, hydrogen, and water do not displace ethanol from the ZnO surface.

Field Effects on Reaction Rate

The reaction rates and yields were not affected by the presence of either positive or negative fields up to the maximum intensity of 1.2×10^4 V/cm in the temperature range above 225°C. This contrast with prior work with ZnO–Cu_2O (*19*) appears due to the different electronic properties of

ZnO and to the fact that the catalyst surface itself was charged in (*19*) while the ZnO films remained electrically neutral in this work. Since there can be no doubt about the large changes in conductivity and rates of adsorption and desorption produced by external field application (Fig. 8 and 9), the insensitivity of reaction rate to field indicates that the rate-limiting step in the dehydrogenation is a surface reaction step which is not affected by the surface concentration of free electrons.

Interpretation

We have pointed out that strong and weak types of ethanol chemisorption are indicated by the temperature dependence of conductivity changes. The weak adsorption can be visualized as hydrogen bonding between the alcohol OH and a lattice O^{2-} ion, while strong adsorption occurs on interstitial Zn_i^+, *viz.*:

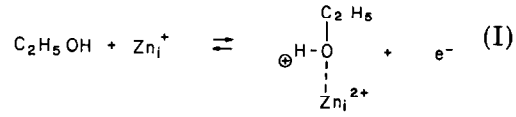

(I)

Such adsorption can be termed "donor-like" since the free electron is generated in the adsorption process rather than supplied by the adsorbate. The valence electron of the interstitial Zn_i^+ is promoted to the conduction band and increases the conductivity. The dehydrogenation step, which is rate-limiting, involves the hydrogen bonded alcohol:

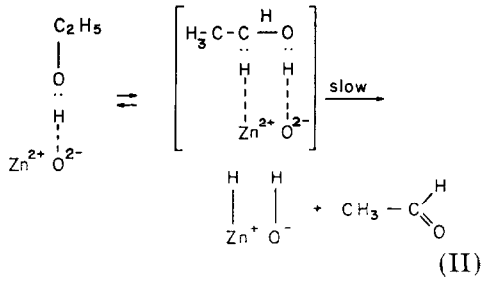

(II)

The (Zn^+–H) complex may either dissociate or desorb hydrogen. In the first case:

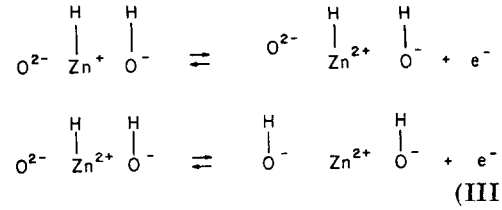

(III)

The donor-like adsorption, step (I), and the dissociation steps (III) form the composite adsorbate layer which behaves as an electron donor. At lower temperatures weak chemisorption predominates, the surface coverage of donor species is small and conductivity changes are small. As temperature increases the fraction of strongly adsorbed donor species increases, particularly hydrogen, and increasingly large conductivity changes are observed. For hydrogen desorption:

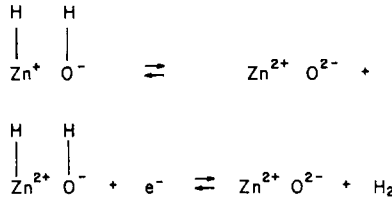

(IV)

These desorption steps compete with the dissociation steps (III) and react oppositely to the presence of free electrons. Negative fields increase e^- concentration, retard the $Z(n^+–H)$ dissociation of (III) and the donor-like adsorption (I), and thus decrease conductivity. The opposite holds for positive fields. Hydrogen desorption, according to this view, would be enhanced by a negative field, corresponding to increases in the concentration of [Zn^+–H] and [Zn^{2+}–H] and decreases in conductivity. All of these effects are observed experimentally

The surface concentration of donor species, ethanol and hydrogen, can be estimated from changes in catalyst conductivity. The resistance ratio (R_0/R_∞) between initial and final conditions is given by:

$$R_0/R_\infty = \sigma_\infty/\sigma_0 = [\mu'_e(n_0 + n_d)]/\mu_e n_0, \quad (1)$$

where σ_0 and σ_∞ are the initial and final values of the catalyst conductivity, n_0 is the initial concentration of electrons and n_d the additional number per unit volume

resulting from the donor species. We will in general not be able to distinguish between electron mobilities before and after adsorption, μ_e and μ'_e, respectively, so n_d can be determined directly from (R_0/R_∞) if n_0 is known. From the initial resistance measurement:

$$n_0 = \sigma_0/q\mu_e = L/aq\mu_e R_0, \qquad (2)$$

where L is the length of the catalyst film test section and a is the film cross sectional area (width by thickness). The value of q is 1.6×10^{-19} C for resistance in ohms, dimensions in cm and mobility in cm²/V-sec. The value of μ_e to use in Eq. (2) is not clearly established. Intemann and Stockmann (*30*) have reported a value of approximately unity for ZnO films in the range of 20–200°C, and Lee and Mason (*31*) a value about two orders of magnitude smaller in their interpretation of the data of Cimino *et al.* (*2*). In fact, the substance of the discussion below is not qualitatively affected by this difference, and the results presented correspond to the ZnO film mobility. Estimates of mobility following Thomas and Lander (*32*) for single crystal ZnO, on the order of 10^2 cm²/V-sec, do not provide a reasonable interpretation of the present data either in terms of boundary layer thickness or donor species concentration. Electron concentrations, n_0, determined from Eq. (2), for the ethanol adsorption experiments from 25–205°C are given in Table 1.

TABLE 1
ZINC OXIDE CONDUCTIVITY AND ELECTRON CONCENTRATION DATA DETERMINED FROM FOUR-POINT RESISTANCE MEASUREMENTS

Temperature (°C)	R_0 (ohm)	σ_0 (ohm-cm)$^{-1}$	n_0 (electrons cm^{-3}) $\mu_e \approx 1$(*30*)
25	6.75×10^7	6.70×10^{-4}	4.2×10^{15}
101	1.20×10^7	3.77×10^{-3}	2.4×10^{16}
150	3.15×10^6	1.44×10^{-2}	9.0×10^{16}
188	7.25×10^5	6.25×10^{-2}	3.9×10^{17}
201	3.69×10^5	1.23×10^{-1}	7.7×10^{17}
205	3.09×10^5	1.47×10^{-1}	0.9×10^{18}

TABLE 2
RESISTANCE RATIOS AND CALCULATED DONOR SPECIES CONCENTRATION FROM ADSORPTION-CONDUCTIVITY EXPERIMENTS

Temperature (°C)	R_0/R_∞	C_{ds} (cm^{-2})
101	2.22	1.1×10^{11}
150	3.57	7.8×10^{11}
201	10.00	1.7×10^{12}

For the conditions of these experiments the concentration of donor adsorbate species on the surface can be determined from the measured resistivity (conductivity) change by (*31*):

$$\Delta\sigma/\Delta\sigma_0 = C_{ds}/xn_0 = (R_0/R_\infty) - 1, \qquad (3)$$

where x is the characteristic crystallite dimension. In Table 2 are given values of C_{ds} computed from resistance ratio measurements on ethanol adsorption at 101, 150, and 201°C (Fig. 4). The X-ray crystallite dimension of 350 Å has been used for x; if the total film thickness is used, C_{ds} values about an order of magnitude smaller are obtained. In either case, the donor concentration decreases sharply with temperature, in agreement with the concept of predominant weak chemisorption at lower temperatures.

It is possible further to obtain a rough comparison between this total donor concentration and the number of interstitial Zn_i^+ ions at the surface. This relationship between free electron concentration and impurity Zn_i^+ concentration is (*33*):

$$n^2/(N_D - n) = (2\pi mkT/h^2)^{3/2} \exp(-E_D/kT), \qquad (5)$$

where N_D is the impurity concentration, n the total free electron concentration, and E_D the energy required to promote an electron from the donor impurity level to the bottom of the conduction band. For ZnO, $E_D = 0.05$ eV (*34*, *35*). At 201°C, using the values of n_0 in Table 1 and Eq. (5) we have:

$$N_D \approx 1.4 \times 10^{18} \text{ cm}^{-3}.$$

Hahn (*36*) and Scharowsky (*37*) report values of N_D (Zn_i^+) for ZnO ranging from 10^{15} to 10^{19} cm^{-3}. The majority of donor impurities are singly ionized for $T > 300$ °K, so the value of N_D is approximately the interstitial Zn_i^+ concentration. Lattice Zn^{2+} concentration is 2.1×10^{22} cm^{-3} (*38*), and the ratio $(Zn_i^+/Zn^{2+}) \approx 10^{-5}$. If this also pertains to the surface, a norm of 10^{15} cm^{-2} for the surface concentration of lattice Zn^{2+} gives a surface interstitial zinc concentration of the order of 10^{10} cm^{-2} at 200°C. The surface concentration of donor adsorbate species at 200°C is (Table 2) about three orders of magnitude greater than this value and may be larger since 10^{15} cm^{-2} is an upper limit for lattice Zn^{2+} concentration. This suggests that the majority of the donor species are hydrogen as in dissociation step (III). The fractional coverage of donor-adsorbed ethanol is small at 200°C, so under these conditions interstitial Zn_i^+ adsorption sites appear to play a relatively minor role in the overall adsorption–reaction mechanism.

Acknowledgments

This work was supported by the National Science Foundation under Grant GK-81 and by Fellowship assistance from Yale University.

References

1. Cimino, A., Molinari, E., and Cipollini, E., *Actes Congr. Int. Catal. 2nd* **1960,** 263 (1961).
2. Cimino, A., Molinari, E., Cramarossa, F., and Ghersini, G., *J. Catal.* **1,** 275 (1962).
3. Molinari, E., Borgianni, C., Liuti, G., and Manes, L., *La Ricerca Sci.* **7,** (3), 647 (1964).
4. Kubokawa, Y., and Toyama, O., *J. Phys. Chem.* **60,** (7), 833 (1956).
5. Bhattacharyya, S. K., De, K. S., and Chrandrashekhar, G. U., *J. Ind. Chem. Soc.* **45,** (6), 512 (1968).
6. Narayanna, D., Subrai-Manyan, V. S., Lal, J., Ali, M. M., and Kesavulu, V., *J. Phys. Chem.* **74,** (4), 779 (1970).
7. Bozon-Verduraz, F., Arghiropoulo, B., and Teichner, S. J., *Bull. Soc. Chim. Fr.* **8,** 2854 (1967).
8. Bhattacharyya, S. K., De, K. S., Pandao, S. N., and Chrandrashekhar, G. U., *Proc. 3rd Int. Cong. Catal.* **1964,** 474 (1964).
9. Bielanski, A., *in* "Catalysis and Chemical Kinetics" (A. A. Balandin, ed.). p. 93, Academic Press, New York, 1964.
10. Bielanski, A., Deren, A. J., and Haber, J., *Nature (London)* **179,** 668 (1957); Bielanski, A., and Sloczynski, J., *Actes Congr. Int. Catal. 2nd* **1960,** 1653 (1961).
11. Derjagiun, B., *Acta Physicochim. USSR* **2,** 377 (1935).
12. Hoenig, S. A., and Lane, J. R., *Surf. Sci.* **11,** 163 (1968).
13. Ivankiv, L. T., and Muzychuk, A. M., *J. Phys. Chem. USSR,* **42,** (2), 223 (1968).
14. Mikheeva, E. P., and Keier, N. P., *Kinet. Catal.* **5,** (4), 668 (1964).
15. Keier, N. P., Mikheeva, E. P., and Usol'Teva, L. M., *Kinet. Catal.* **8,** (5), 1018 (1967).
16. Stadnik, P. M., and Sekeresh, E. Yu., *Kinet. Catal.* **5,** (3), 375 (1964).
17. Stadnik, P. M., and Fentsik, V. P., *Kinet. Catal.* **2,** (4), 509 (1961).
18. Dmitrenko, L. M., Lachinov, S. S., and Sibyakova, R. F., *Kinet. Catal.* **1,** (3), 352 (1960).
19. Ivankiv, L. I., Miliyanchuk, M. V., and Filatove, A. K., "Thesis of the All-Union Conference on the Deep Mechanism of Catalytic Reactions," p. 81, Moscow, 1964.
20. Lee, V. J., *Science* **152,** 514 (1966).
21. Hsu, W., and Lee, V. J., presented: AIChE New York Meeting, November, 1967.
22. McArthur, D. P., Ph.D. dissertation, Yale University, 1971.
23. Dabrowski, J. E., Ph.D. dissertation, Yale University, 1969.
24. Seitz, G., Ph.D. dissertation, Universität Erlangen-Nürnberg, 1955.
25. Rhodin, T. W., *J. Amer. Chem. Soc.* **72,** 4343 (1950).
26. Adkins, H., and Lazier, W. H., *J. Amer. Chem. Soc.* **46,** 2291 (1924); **48,** 1671 (1926).
27. Lazier, W. A., and Adkins, H., *J. Amer. Chem. Soc.* **47,** 1719 (1925).
28. Liashenko, V. I., and Litovchenko, V. G., *Sov. Phys. Tech. Phys.* **3,** (3), 429 (1958).
29. Taylor, H. A., and Thon, N., *J. Amer. Chem. Soc.* **74,** 4169 (1952).
30. Intemann, K., and Stockmann, F., *Z. Physik.* **131,** 10 (1951).
31. Lee, V. J., and Mason, D. R., *J. Appl. Phys.* **35,** (5), 1557 (1964).
32. Thomas, D. G., and Lander, J. J., *J. Chem. Phys.* **25,** 1136 (1956).
33. Mott, N. F., and Gurney, R. W., "Electronic

Processes in Ionic Crystals," p. 158. Clarendon Press, Oxford, 1940.
34. HARRISON, S. E., *Phys. Rev.* **93,** 52 (1953).
35. HUTSON, A. R., *Bull. Amer. Phys. Soc.* **1,** Series 2, 381 (1956).
36. HAHN, E. E., *J. Appl. Phys.* **22,** (7), 855 (1951).
37. SCHAROWSKY, E., *Z. Physik* **135,** 318 (1953).
38. HEILAND, G., *Solid State Phys.* **8,** 195 (1959).